2014 based MMCs: Properties improvement by $(TiCN)_p$ and trace additions

E. M. RUIZ-NAVAS*, M. L. DELGADO, J. M. TORRALBA
Materials Science and Engineering Department, Universidad Carlos III de Madrid, C/Avenida de la Universidad, 30, 28911, Leganés, Spain
E-mail: emruiz@ing.uc3m.es
E-mail: mdtienda@ing.uc3m.es
E-mail: torralba@ing.uc3m.es

Published online: 10 April 2006

Sintering of aluminum alloys is usually performed by the formation of a liquid phase. A liquid phase in 2xxx series alloys is formed from α+Al_2Cu eutectic. In this work, the influences of trace elements like Sn or Pb, and the addition of a ceramic reinforcement, such as TiCN, on 2014 alloys are studied. Mechanical properties as well as a microstructural study show improved results.

1. Introduction

Supersolidus liquid phase sintering involves sintering of a prealloyed powder at a temperature between the solidus and the liquidus to give a liquid phase, which results from the partial melting of the solid phase. Sintering of an aluminum prealloyed powder which belongs to series 2xxx also involves transient liquid phase sintering, due to the formation of the α+Al_2Cu eutectic at 548°C. In the transient liquid phase sintering, the liquid phase has a high solubility in the solid phase. As a consequence, it diffuses into the solid phase and solidifies by diffusional homogenization.

To delay the transient aspect of the liquid phase due to the solubility of copper in the aluminum matrix, some trace elements can be added. It have been shown that some elements (Pb, Sn, Bi, Sb and In) acting by their high vacancy binding energies or modifying the liquid surface tension, can enhance the sintering process. It is possible that the trace element binds with the vacancies in the Al, thereby reducing the rate of Cu diffusion in the Al. This would hinder the dissolution of copper and hence delay the transient aspect of the system. The liquid persists for longer times, thereby improving sintering [1–6]. Also, elements like Sn and Pb diminish the liquid surface tension, modifying the contact angle and improving, therefore, the sintering process. On the other hand, it has been concluded that the presence of TiCN enhances thermo-mechanical properties of Al-Mg_2Si cast alloys [7, 8]. Adding TiCN to 2014 alloy, the behaviour expected from the metal matrix composite formed would be a combination of the great strength of the ceramic while avoiding the brittle failure and the ductility of the metals. Nevertheless, it could be also expected a decrease on the material densification, as a consequence of the impossibility of sintering the metal particles and the ceramic particles [9–11]. In this paper the influence of Sn, Pb and TiCN addition on the liquid phase, and hence, on the sintering process of an Al-Cu-Mg-Si alloy is reviewed.

2. Experimental

The compositions of the powders employed are shown in Table I. Powder alloys were prepared by mixing the 2014 alloy powder with the Sn or Pb powders and/or the TiCN powder for 30 min in a Turbular powder mixer. The compositions of the alloy studied are shown in Table II.

Compaction of the specimens was performed using a hydraulic press and a floating flexural strength die. The die lubricant employed was zinc stearate. Specimens were pressed to reach ≈85% of green density, using a pressure of 400 MPa. The sintered density was determined using the Archimedesś method, and the densification Ψ, was calculated to determine the amount of shrinkage or expansion:

$$\psi = \frac{\rho_s - \rho_g}{\rho_t - \rho_g} \quad (1)$$

where ρ_s, ρ_g and ρ_t are the sintered, green and theoretical density, respectively. A positive value of Ψ indicates shrinkage; Ψ approaches unity as full density is attained.

*Author to whom all correspondence should be addressed.
0022-2461
DOI: 10.1007/s10853-005-5680-7

TABLE I Characteristics of the as-received powders

Powder	Source	Size fraction (μm)	Element	%
AA2014	Aluminum Powder Company	<75	Cu	4.4
			Mg	0.4
			Si	0.7
			Al	bal.
TiCN	H.C. Starck	1.0–1.3	C_{TOTAL}	9.3–10.3
			C_{FREE}	0.05 Max.
			N	10.3–11.3
			O	1.5 Max.
Sn	Goodfellow	<45		99.75
Pb	Goodfellow	<45		99.9

TABLE II Compositions of the alloys studied

Base alloy	% wt Sn	%wt Pb	%wt TiCN
2014	–	–	–
2014	0.15	–	–
2014	–	0.15	–
2014	–	–	5
2014	0.15	–	5
2014	–	0.15	5

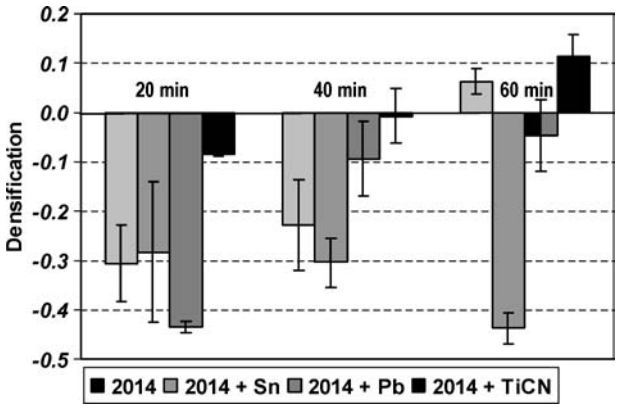

Figure 1 Densification values obtained for 2014 alloy, 2014+Sn alloy, 2014+Pb alloy and 2014+TiCN alloy, sintered for different times.

Sintering and delubrication occurred in a horizontal furnace with a gas mixture of H_2 (4.98%)-N_2 (bal.). The heating rate for dewaxing was 10°C min^{-1}, until the furnace reached 300°C. The temperature was maintained for 30 min for dewaxing. After that, the samples were heated to 570°C at a heating rate of 10°C min^{-1}. At this point, the temperature was maintained for 20, 40 or 60 min. A complete microstructural study was made by scanning electron microscopy (SEM). Hardness of the samples was evaluated by Vickers indentation using a 30 kg load. Bending strength was carried out following MPIF standard 41.

3. Results

3.1. Densification and microstructure

The obtained results for the densification of the alloys are represented in Fig. 1. Additions of Sn, Pb and TiCN to 2014 alloy cause different effects on the alloys densification. As can be seen in Fig. 1, 2014 alloy experiences a decrease in the swelling which is produced by the liquid phase formation and its influence on the wetting angles, when the sintering time is increased. When the sintering time is 60 min, the densification value is above zero. The addition of TiCN to the alloy increases the densification value compared to 2014 alloy (after 60 min of sintering), opposite to what was expected. This enhancement of the densification parameter can be checked by the evolution of the microstructure.

Although 2014 alloy densification value is increased with longer sintering time, it is clear that the alloy after 60 min of sintering time does not look properly sintered (Fig. 2). The main reason could be an inadequate diffusion of aluminium through the liquid phase during the sintering process. In the figure, the light areas correspond to copper rich zones, coming from the liquid formed during the sintering process, and the aluminum particles can be identified as the grey particles.

However, the opposite behaviour (analysing the densification parameter) can be observed for 2014 + 0.15 wt.% Sn alloy, also represented in Fig. 1. As can be seen in this figure, Sn addition does not aid 2014 densification; as sintering time is increased, densification values decrease. Densification values are negative, indicating swelling, at every time investigated. Looking at the microstructures obtained for the alloy sintered for 20, 40 and 60 min respectively (Fig. 3), it can be seen how the porosity is high in all the microstructures obtained, and how the copper rich zones are not homogeneously distributed between the aluminum particles.

If 2014 + 0.15 wt% Pb alloy sintering behaviour is now analysed through the densification parameter in Fig. 1, it can be seen that this alloy exhibits a different densification evolution with the sintering time if it is compared to the alloy in which Sn is added. After 60 min of sintering time, densification reaches a value close to zero.

Through the analysis of the microstructure (Fig. 4), it is clear that the densification process is aided when the sintering time is increased. The porosity of the samples diminishes at the same time as the aluminum particles are closer to each other. Looking at the copper rich areas, the liquid phase diffusion seems to be more homogeneous, filling the pores between the aluminum particles. The Pb addition affects material densification through modification of the liquid phase. Instead of the behaviour observed when Sn is added to the 2014 alloy, Pb addition can aid material densification and, as a consequence, improve the sintering process.

Analysing now the influence of the ceramic reinforcement addition, TiCN, on the alloy densification (Fig. 1), it can be firstly pointed out that densification is always improved for all the sintering times studied. 2014 + 5 wt% TiCN material reaches better densification values compared to 2014 + 0.15 wt% Sn and 2014 + 0.15 wt% Pb alloys. After 40 min of sintering time, the alloy is shrinking. After 60 min, the alloy reaches the highest densifica-

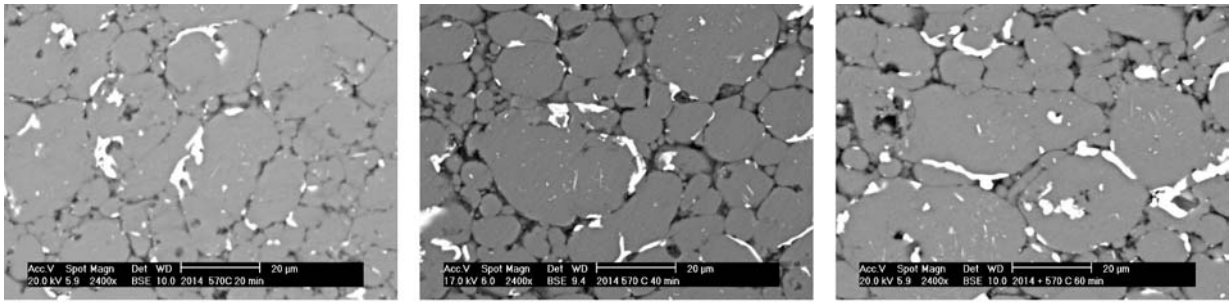

Figure 2 2014 alloy microstructure evolution with the sintering time.

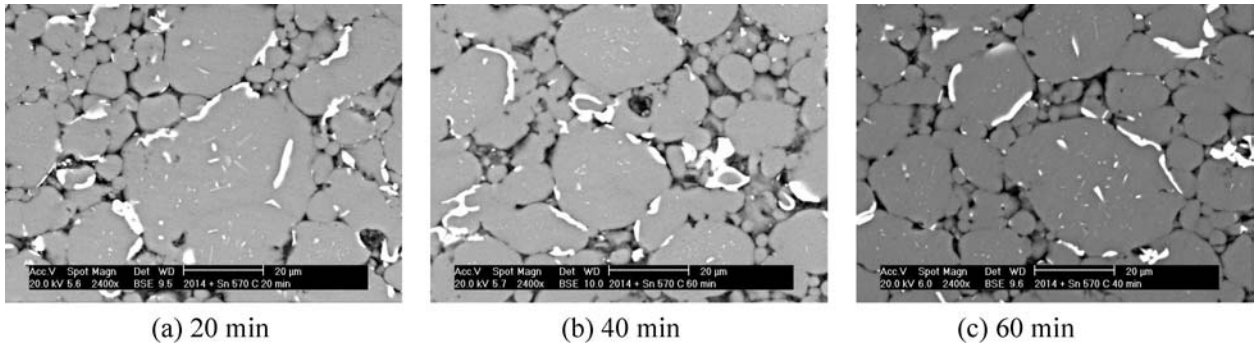

Figure 3 2014+0.15 wt% Sn alloy microstructure evolution with the sintering time.

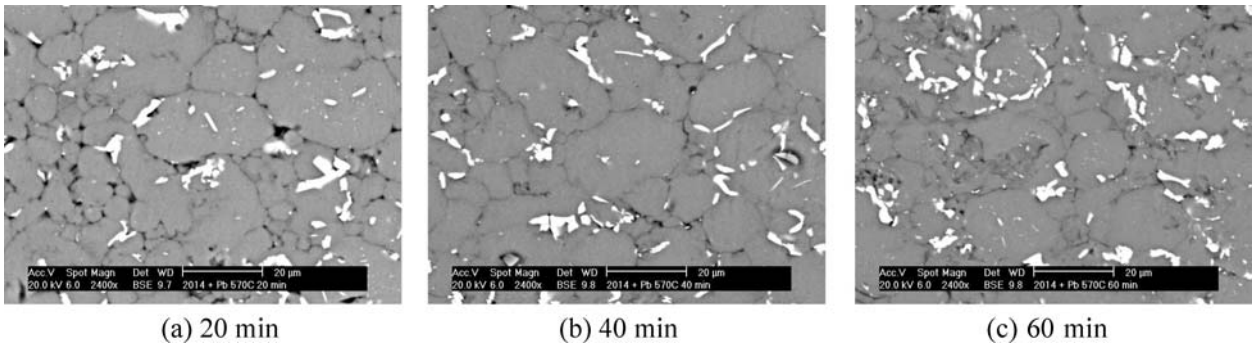

Figure 4 2014+0.15 wt% Pb alloy microstructure evolution with the sintering time.

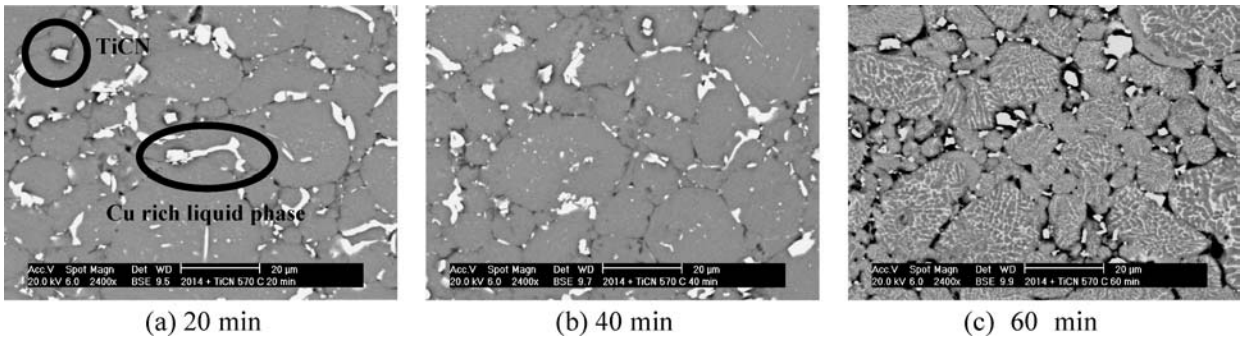

Figure 5 2014+5 wt% TiCN alloy microstructure evolution with the sintering time.

tion value of all the alloys. It is clear that the addition of the ceramic reinforcement has a positive effect on the material densification, which would affect the rest of the measured properties.

2014 + 5 wt% TiCN alloy microstructure is shown in Fig. 5. In the microstructures, the ceramic reinforcement can be identified as bright zones. After 20 min of sintering time, the material porosity is reduced compared to the

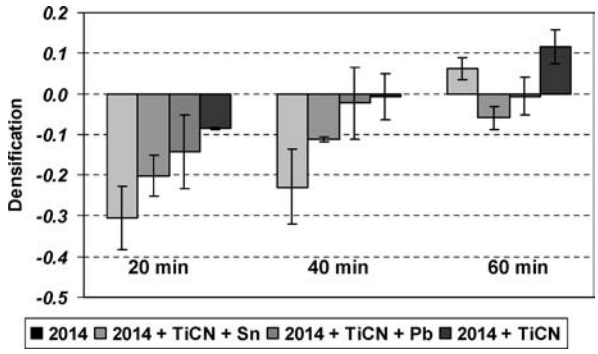

Figure 6 Densification values obtained for 2014 alloy, 2014+5 wt% TiCN+0.15 wt% Sn, 2014+5 wt% TiCN+0.15 wt% Pb alloy and 2014+5 wt% TiCN, sintered for different times.

rest of alloys (Figs 2(a), 3(a) and 4(a)). The main difference can be observed when a sintering time of 60 min is employed, the copper rich zones are completely located inside the aluminum particles.

The influence on densification of Sn and Pb additions to 2014 alloy reinforced also with TiCN is shown in Fig. 6. The densification values for 2014 + 0.15 wt% Sn+5% TiCN and 2014+0.15 wt% Pb+5% TiCN alloys are shown in comparison to 2014 and 2014+5 wt% TiCN alloys (Fig. 6).

As can be seen in Fig. 6, densification is improved for both alloys (2014+5 wt% TiCN+0.15 wt% Sn and 2014+5 wt% TiCN+0.15 wt% Pb) when the sintering time is increased. The densification values obtained when Pb and Sn are added are always between the ones obtained in the case of 2014 and 2014+5 wt% TiCN alloys sintered for 20 and 40 min. However, when longer sintering times are employed, the obtained densification values (Fig. 6) reveal shrinkage for the 2014 and 2014+5 wt% TiCN alloys but swelling for the 2014+5 wt% TiCN+0.15 wt% Sn and 2014+5 wt% TiCN+0.15 wt% Pb alloys.

The microstructural evolution with sintering time of 2014+5 wt% TiCN when Sn and Pb are added is shown in Fig. 7.

If the influence of Sn and TiCN additions to 2014 base alloy on the microstructure is studied in Figs 3(c) and 7(c) respectively, differences can be seen in the obtained microstructure due to the reinforcement addition. In Fig. 7(c) where both TiCN and Sn, are added, the microstructure is a single compact body. The aluminum particles are bounded by TiCN particles and copper rich zones. The copper rich zones appear more homogeneously distributed compared to the rest of alloys microstructures and the porosity has been widely reduced. The sintering process appears more advanced than in 2014+0.15 wt% Sn case after the same sintering time (Fig. 7). Bonding between particles reveals a better sintering process compared to microstructures where the aluminum particles can be perfectly distinguished.

However the differences in the microstructures between 2014+0.15 wt% Pb and 2014+5 wt% TiCN+0.15 wt% Pb are not so marked (Figs 4(c) and 7(c) respectively). Microstructurally, important differences can not be detected.

3.2. Bending strength and hardness

Hardness and bending strength are represented in Figs 8 and 9, respectively. As can be seen in these figures the

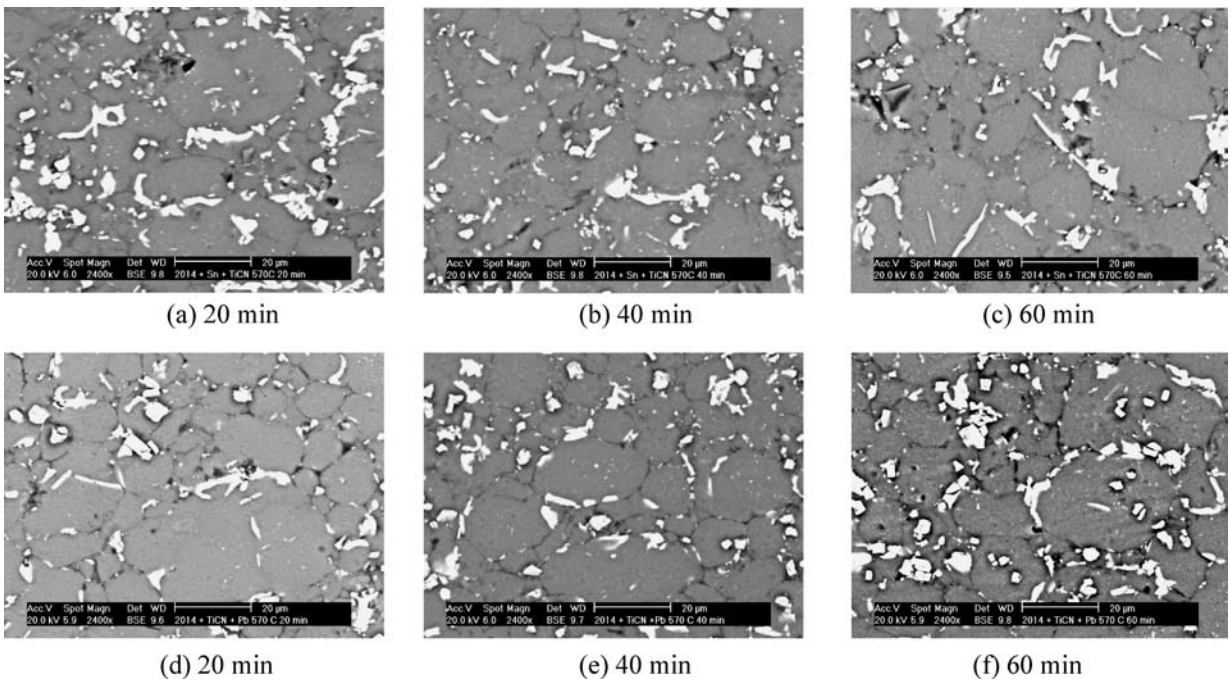

Figure 7 Microstructure evolution with the sintering time of 2014+5 wt% TiCN+0.15 wt% Sn (a), (b), (c) and 2014+5 wt% TiCN+0.15 wt% Pb alloys (d), (e), (f).

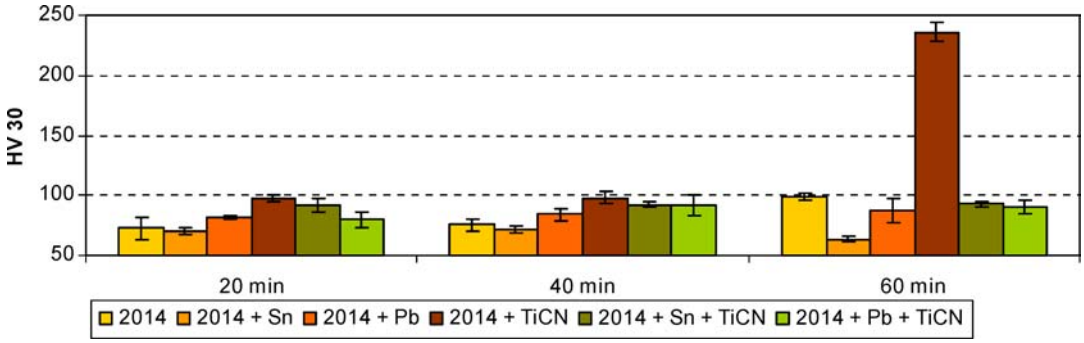

Figure 8 Alloys hardness evolution with sintering time.

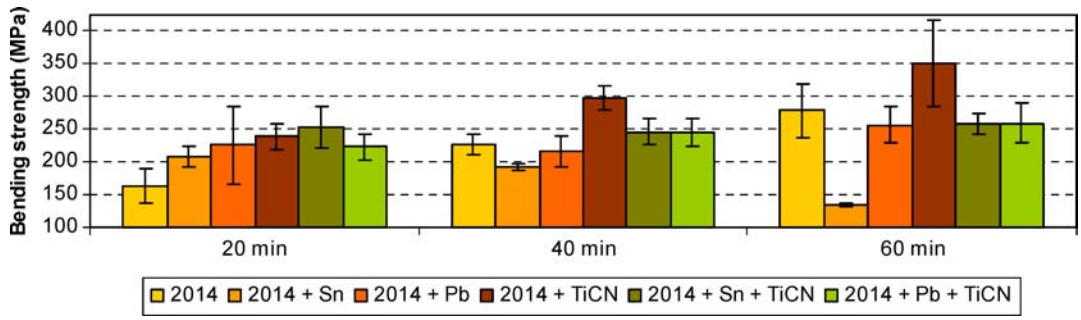

Figure 9 Alloys bending strength evolution with sintering time.

tendency is the same as shown above for the densification parameter; when the sintering time is longer, the hardness is also increased, except for the 2014+0.15 wt% Sn alloy, for which hardness decreases with the sintering time. The distribution of the copper rich zones and the high porosity level not only affects densification, but consequently influences hardness and bending strength. The highest hardness value is from 2014+5 wt% TiCN after 60 min of sintering time. MMCs are reported to present improved properties since these materials combine metallic with ceramic properties [12–15]. The addition of both ceramic particles and trace elements cause intermediate values in hardness, compared to 2014, 2014+0.15 wt% (Pb, Sn) and 2014+5 wt% TiCN. The combination of trace elements and ceramic enhances properties compared to the alloy without reinforcement but decreases properties compared to MMC. The same tendency can be observed in the bending strength of the samples, shown in Fig. 9, where the best results are obtained for the metal matrix composite based in 2014 and reinforced with TiCN.

4. Discussion

In order to explain how the addition of the trace elements, like Sn, can affect the material densification and mechanical properties, several explanations have been given. One of them explains how elements like Sn diffuse into the Al matrix ahead of the copper. This ties up the vacancies and delays the transient aspect of the liquid phase during sintering [2]. On the other hand, it has been reported [1, 2, 5, 6] that Sn additions can enhance prealloyed powders sintered properties. Sn and Pb were added to prealloyed alloys, 2124 and 6061, improving sintering. The mechanism of how trace additions aid the sintering of 2xxx series aluminum alloys was explained by means of the reduction of the liquid phase surface tension. Sn and Pb trace additions promote changes in the distribution and spreading of the liquid during sintering. When Sn and Pb are melted in the liquid phase (230°C and 330°C are the melting points, respectively) according to the Gibbs adsorption isotherm and due to their low surface tension, these components will segregate to the surface of the liquid.

The reason why these melted elements segregated on the liquid surface could improve sintering is related to the liquid wetting and the contact angle. To enhance liquid phase sintering, the most important factor is the liquid spreading. The liquid spreading is determined by the wetting angle (θ), given by the Young's equation [16]:

$$\gamma_{lg} \cos\theta = \gamma_{sg} - \gamma_{sl} \tag{2}$$

where γ_{lg} liquid-gas surface tension, γ_{sg} solid-gas surface tension, γ_{gl} solid-liquid surface tension. From expression (2) when a liquid wets a solid ($\theta < 90°$) all the factors that reduce the liquid-gas or the solid-liquid surface tension will reduce the contact angle, which consequently means a better spreading, densification and finally the improvement of sintering. Looking at the data shown in Table III, the trace elements, which present lower surface energy, are supposed to diminish the surface tension of the liquid (since these elements would segregate to the liquid surface), improving the wetting of the liquid phase to the

TABLE III Surface tension values measured at melting point

Composition	Surface tension ($N\ m^{-1}$)	Element	Surface tension ($N\ m^{-1}$)
Al (99.54%)-Sn(0.46%) [17]	0.797*	Sn [16]	0.544
Al (99.84%)-Pb(0.16%) [17]	0.573*	Pb [16]	0.468
Al (82.7%)-Cu (17.3%) [18]	0.160	Cu [16]	1.36

*Surface tension calculated at the sintering temperature (570°C).

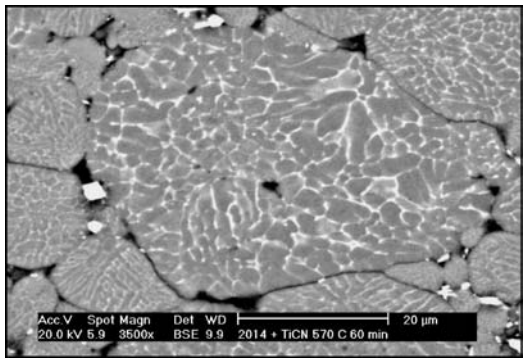

Figure 10 Particle detail of 2014+5% TiCN sintered for 60 min.

aluminum particles and as a consequence, sintering. It is important to note that surface tension of liquid Pb is lower than liquid Sn, and also, when both elements are added to aluminum in the same percentage, the surface tension of the liquid alloy with Pb is also lower than the liquid alloy with Sn [17].

Looking at the results shown above, it can be seen that Sn additions to 2014 do not improve the mechanical properties. Analysing the results obtained and the samples microstructures, it can be concluded that Sn additions do not aid the sintering of 2014 alloy. However, the solubility of Sn in aluminium may be high enough at the sintering temperature so that the amount of free Sn is insufficient to reduce the liquid's surface tension preventing the beneficial effect from being detected [6]. It is important to note that the solubility of Sn in Al is approximately 0.11% at 570°C [19] and only 0.15 wt% of Sn has been added to 2014 alloy.

However, Pb additions to 2014 alloy improved densification and mechanical properties if they are compared to the results obtained for 2014+0.15 wt% Sn alloy. Nevertheless, Pb additions did not improve the sintered properties if they are compared to those of the 2014 alloy. The quantity of Pb addition could have also been insufficient to enhance the mechanical properties compared to the 2014 alloy. The improved results of Pb additions compared to Sn additions could be expected due to the lower solubility of Pb in aluminum and its lower surface tension. Hence, Pb addition could be expected to be more effective, as can be observed in parameters such as densification and hardness.

The influence of the ceramic reinforcement should be also analysed. The main difference with the other materials can be detected in the microstructure obtained after 60 min of sintering time (Fig. 5c). In this micrograph, the copper rich zones are completely inside the aluminum particles. The appearance of the copper rich zones inside the aluminum particles (for 2014+5% TiCN) can be observed with more detail in Fig. 10.

After 60 min of sintering time, as it is shown in Fig. 10 copper rich zones are inside the aluminium particles among the former aluminum grain boundaries. It could be possible that TiCN particles aid the liquid diffusion inside the aluminum particles, making easy the liquid diffusion between the grain boundaries. The TiCN particles may help to break the aluminum oxide layer that covers the aluminum particles during the pressing step. When the sample is heated and the liquid phase is formed, this liquid could diffuse between the particles through the broken oxide layer into the particles. A schematic where the possible broken points could be located after compaction is shown in Fig. 11.

It is also important to point out the possible effect derived from the lack of wettability between melted aluminum and TiCN. The contact angle of liquid aluminum on TiCN is always above 90° in the 720°–900°C temperature range. Although the alloy employed is not pure aluminum and the sintering temperature is not in this range, it has been proven that Si or Si and Mg added to aluminum do not significantly improve the wetting of TiCN by aluminum [8]. It is possible that the combination of both factors, one, the disrupted aluminum oxide layer together with the unwettability of the liquid on the TiCN, promotes the liquid phase diffusion into the aluminum particles.

It is important to remark that the importance of the TiCN additions is not only related to an increase in the material densification since the ceramic improved both hardness and bending strength of the aluminum alloys. Materials containing the ceramic reinforcement show enhanced mechanical properties than the base alloys, probably due to

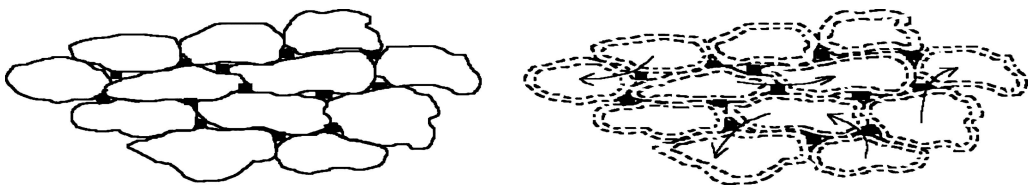

Figure 11 Compacted body showing the possible oxide layer breaking points and TiCN particle location.

the combination of ceramic and metallic properties [12–15].

5. Conclusions

- TiCN particles added to 2014 alloy increased material densification and mechanical properties.
- Sn did not improve densification or mechanical properties when it was added to the 2014 alloy. However, Pb additions enhanced properties when it was sintered for 40 min. Neither Sn nor Pb enhanced material properties probably due to an insufficient quantity of element added compared to the element solubility in aluminum
- Alloys with trace elements and ceramic additions exhibit intermediate values of the measured properties

Acknowledgments

The authors would like to thank CICYT MAT2000-0442-C02-01 project and FPI Program of Comunidad Autónoma de Madrid for financial support to realise this work

References

1. G. B. SCHAFFER, S. H. HUO, J. DRENNAN and G. J. AUCHTERLONIE, *Acta. Mater.* **49** (2001) 2671.
2. T. B. SERCOMBE and G. B. SCHAFFER, and *ibid.* **47–2** (1999) 689.
3. R. N. LUMLEY and G. B. SCHAFFER, *Scripta Mater.* **39** (1998) 1089.
4. D. P. BISHOP, J. R. CAHOON, M. C. CHATURVEDI, G. J. KIPOUROS and W. F. CALEY, *Mater. Sci. Eng. A* **290** (2000) 16.
5. T. B. SERCOMBE and G. B. SCHAFFER, and *ibid.* **268** (1999) 32.
6. T. B. SERCOMBE, *ibid.* **341** (2003) 163.
7. G. LEVI, W. D. KAPLAN and M. BAMBERGER, *ibid.* **326** (2002) 288.
8. G. LEVI, M. BAMBERGER and W. D. KAPLAN ACTA MATERIALIA, **47**(14) (1999) 3927.
9. R. MITRA and Y. R. MAHAJAN, *Defence Sci. J.* **43–4** (1993) 397.
10. T. P. D. RAJAN, R. M. PILLAI and B. C. PAI, *J. Mat. Sci.* **33** (1998) 3491.
11. V. ESCUDER, V. AMIGÓ, F. ROMERO, A. BAUTISTA and J. M. TORRALBA, 8th Nacional Congress of Solid Mechanical Properties,(2002). Valencia – Spain, 477.
12. L. E. G. CAMBRONERO, E. SÁNCHEZ, J. M. RUIZ-ROMAN and J. M. RUIZ-PRIETO, *J. Mater. Processing Tech.* **143–144** (2003) 378.
13. SOON-JIK HONG, HONG-MOULE KIM, DAE HUH, C. SURYANARAYANA and BYONG SUN CHUN, *Mater. Sci. and Eng.* **347** (1–2) (2003) 198.
14. K. B. LEE, H. S. SIM, S. W. HEO, H. R. YOO, S. Y. CHO and H. KWON, *Composites Part A: Applied Science and Manufacturing* **33** (5) (2002) 709.
15. C. E. DA COSTA, W. C. ZAPATA, F. VELASCO, J. M. RUIZ-PRIETO and J. M. TORRALBA, *J. Mat. Processing Tech.* **92–93**, (1999) 66.
16. Wetability, Berg J.C. (1993) 6.
17. L. GOUMIRI, J. C. JOUD, P. DESRE and J. M. HICTER, *Surface Science.* **83** (1979) 471.
18. N. MARASLI, D. J. HUNT, *Acta Materalia.* (1996) 1085.
19. ASM. HANDBOOK, *American Society of Metals.* **3** (1984–1994) 2.

Received 13 April
and accepted 25 July 2005